

Indirect imaging of the accretion stream in eclipsing polars IV: V895 Cen

Nikita Salvi¹, Gavin Ramsay¹, Mark Cropper¹, D. A. H. Buckley², R. S. Stobie²

¹*Mullard Space Science Laboratory, University College London, Holmbury St. Mary, Dorking Surrey, RH5 6NT*

²*South African Astronomical Observatory, PO Box 9, Observatory 7935, South Africa*

27 October 2018

ABSTRACT

We present spectroscopic and high speed photometric data of the eclipsing polar V895 Cen. We find that the eclipsed component is consistent with it being the accretion regions on the white dwarf. This is in contrast to Stobie et al who concluded that the eclipsed component was not the white dwarf. Further, we find no evidence for an accretion disc in our data. From our Doppler tomography results, we find that the white dwarf has $M \gtrsim 0.7 M_{\odot}$. Our indirect imaging of the accretion stream suggests that the stream is brightest close to the white dwarf. When we observed V895 Cen in its highest accretion state, emission is concentrated along field lines leading to the upper pole. There is no evidence for enhanced emission at the magnetic coupling region.

Key words:

accretion–binaries: eclipsing–stars:magnetic fields–cataclysmic variables–stars: individual: V895 Cen

1 INTRODUCTION

Polars are interacting binaries consisting of a red dwarf secondary and a strongly magnetized ($\sim 10\text{--}200$ MG) white dwarf primary. In these systems the secondary fills its Roche lobe. Material falls under gravity from the secondary towards the primary, initially along the binary orbital plane before the magnetic field of the primary forces it to leave the orbital plane and eventually impacts quasi-radially onto the white dwarf. Unlike non-magnetic cataclysmic variables (CVs) the strong magnetic field of the white dwarf is high enough to prevent the formation of an accretion disc around the primary.

Although our understanding of the accretion flow near the white dwarf is now relatively well understood (eg Wu 2000 and references therein) the region where accretion flow first interacts with the magnetic field of the white dwarf is not. The flow interacts with the magnetosphere in a complex manner and it is not easy to isolate stream emission from other emission sources in the system (which are generally brighter).

Eclipsing systems provide an opportunity to study the accretion flow as a separate and distinct source for a short period of time, when the emission from the bright accretion region on the white dwarf is blocked by the secondary. Light curves of the eclipse contain information about the structure and the brightness distribution along the stream.

The stream brightness distribution can be retrieved using an indirect imaging technique which can reconstruct the brightness of the region between the primary and the secondary.

One such technique is that of Hakala (1995) who devised an indirect imaging method based on Maximum Entropy to deduce the brightness distribution along the accretion stream of HU Aqr. This technique has been developed further by Harrop-Allin et al (1999a, 1999b, 2001) who used a more physically realistic stream trajectory, improving the model’s optimizing algorithm and including the projection effects.

V895 Cen was discovered serendipitously using the EUVE satellite (Craig et al 1996). Craig et al observed strong line emission and low/high brightness states and concluded V895 Cen was likely to be a polar. Its orbital period of $P_{orb}=4.765$ h (Stobie et al 1996) is the second longest period currently known for a polar and the system is found to alternate frequently between high and low accretion states. Stobie et al (1996) concluded that it is an eclipsing polar but that the secondary minimum of the ellipsoidal variation was offset with respect to the eclipse. They suggested the eclipsed component was a hot compact source which appeared to be distinct from the white dwarf, probably associated with the accretion stream. Howell et al (1997) also concluded the eclipse to be of an extended object much larger than the white dwarf, perhaps a partial accretion disc which forms during the high state. Stobie et al (1996) found no ev-

idence for significant levels of polarization in a low accretion state.

To investigate the nature of the eclipsed component, we have applied the techniques of indirect imaging and Doppler tomography to this system to study the spatial and temporal changes in the stream and to determine if the eclipse is associated with the white dwarf or the stream.

2 SPECTROSCOPIC OBSERVATIONS

Low resolution spectra of V895 Cen were obtained with the goal of detecting the presence of cyclotron humps and hence the magnetic field strength of the accreting white dwarf from their spacing. Medium resolution spectra were also obtained with the goal of mapping the location of the line emission regions in the binary system using Doppler tomography.

2.1 High accretion state observations

Spectra were obtained of V895 Cen on 2 and 3 March 1998 using the ANU 2.3 telescope and the double beam spectrograph. The conditions were good and the seeing was $\sim 1\text{--}2''$. Blue and red spectra were taken using the 300 l/mm gratings and the effective wavelength range were 3800–5500Å and 6400–8700Å respectively. Exposure times were 240 sec. With a slit width of 2.0'' the FWHM of the lines in the arc lamp spectra were measured as $\sim 5\text{\AA}$ near H α .

On the first night V895 Cen was observed from $\phi \sim 0.94\text{--}0.30$ (on the ephemeris of Stobie et al 1996) while on the second night we were not able to accurately attach time information due to a computer problem. It was clear, however, that V895 was observed in a high accretion state with prominent emission lines of H and He. There is no convincing evidence for the presence of cyclotron humps in our spectra.

2.2 Low accretion state observations

More spectra were obtained of V895 Cen on 18 April 1998 using the ANU 2.3 telescope and the double beam spectrograph. Some light cloud was present at the start of the night and also towards the end of the night. The seeing was $\sim 1''$. Blue and red spectra were taken using the 600 l/mm gratings resulting in effective wavelength ranges of 3800–5600Å and 5800–7400Å. Exposure times were 520 sec and 500 sec for the blue and red spectra respectively. With a slit width of 1.2'' the FWHM of the lines in the arc lamp spectra were measured as 2.1 Å near H α . A total of 51 fully calibrated spectra were obtained in each arm of the spectrograph.

V895 Cen was found to be in a low accretion state in contrast to our March 1998 observations. The signal to noise ratio of the blue spectra were very low and so we do not discuss these any further. Two of the red spectra are shown in Figure 1. The spectrum taken during $\phi=0.0$ is almost entirely that of the dwarf secondary star. Comparing template spectra of late type dwarf stars we estimate the spectral type of the secondary to be M1–M2 – consistent with the M2 estimate of Stobie et al (1996). Figure 1 also shows the spectrum at $\phi=0.27$. Apart from increased emission at H α the shape and intensity of this spectrum is virtually unchanged

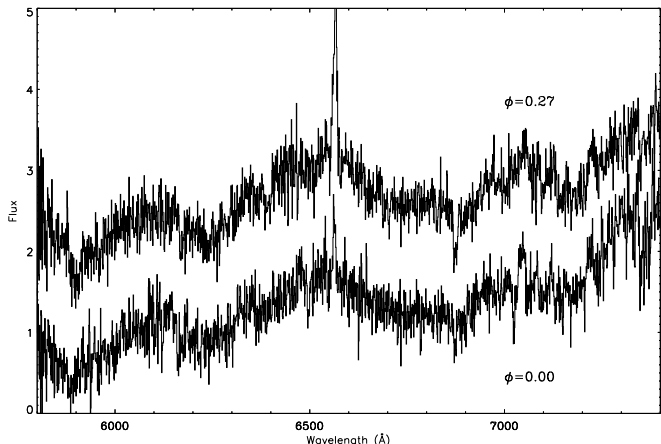


Figure 1. Spectra taken using the ANU 2.3m double beam spectrograph on 18 April 1998 when it was in a low accretion state. Our spectra are phased on the ephemeris in Stobie et al (1996) and we show spectra from two binary orbital phases. The upper spectrum has been displaced vertically by 1.0 flux unit (which is arbitrary). At both phases the spectrum is dominated by the secondary star.

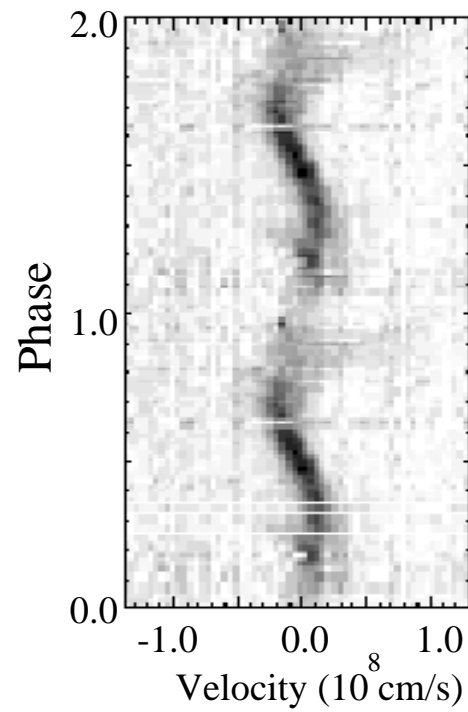


Figure 2. The H α emission line taken on 18 April 2000 folded on the binary orbital period.

from that at $\phi=0.0$. We show the wavelength variation in the spectrum near H α over the binary cycle in Figure 2.

3 DOPPLER TOMOGRAPHY

Doppler Tomography is used to map the accretion flow in binary systems in velocity space. It has been applied to several polars such as HU Aqr (Schwope, Mantel & Horne 1997). Here we use the code of Spruit (1998) to produce a Doppler

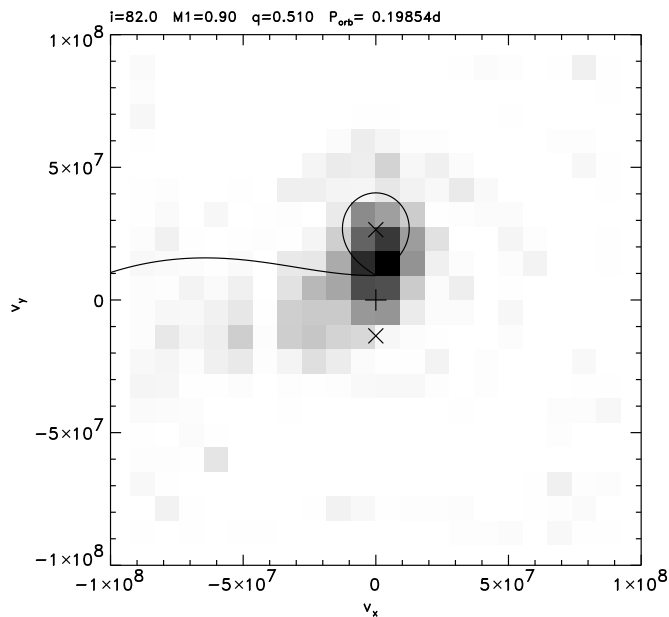


Figure 3. The Doppler map of V895 Cen obtained in April 1998 when it was in a low accretion state made using the $H\alpha$ emission line. The solid curve represents the predicted path of the ballistic trajectory of the accretion stream leaving the L_1 point. We have assumed $M_1=0.9M_\odot$ and $M_2=0.46M_\odot$.

map of V895 Cen. Many Doppler maps of polars show emission from the irradiated face of the secondary star. We can place some constraint on the mass ratio, $q = M_2/M_1$, by varying q and M_1 so that emission is located in the correct location. We can constrain $0.25 \lesssim q \lesssim 0.7$ purely from these maps.

We can constrain M_2 using the secondary mass-orbital period relationship (Warner 1995) and obtain $M_2 \sim 0.46M_\odot$. Although there is some evidence that secondaries in CVs with binary orbital periods greater than 3 hrs have spectral types later than implied by the solar-abundance main sequence for isolated stars, the spectral type for V895 Cen found in §2.2 is consistent with that expected for its binary orbital period (Beuermann et al 1998). Based on theoretical relationships between the radius of the secondary and binary orbital period (Baraffe & Kolb 2000) we estimate the uncertainty on M_2 as $\sim 0.05M_\odot$ for $P_{orb}=4.765$ hr.

In generating our Doppler map we assume a binary inclination of 82° (§6). For $M_2=0.41-0.51$, we find that $M_1 > 0.7M_\odot$ if most of the line emission is located at the irradiated face of the secondary. We show the Doppler map of V895 Cen in $H\alpha$ emission in Figure 3 for $M_1=0.9M_\odot$ and $M_2=0.46M_\odot$. We use a mass of $M_1 = 0.9M_\odot$ for the rest of the paper, implying $q=0.51$.

Although our Doppler map shows that most of the line emission in $H\alpha$ originates at the irradiated face of the secondary star, there is faint emission from a stream component. Compared to systems in a high accretion state (eg HU Aqr), the stream is located at lower V_y than the predicted ballistic trajectory of the stream. There is no evidence for an accretion disc in these spectroscopic data.

4 PHOTOMETRIC OBSERVATIONS

Photometric observations of V895 Cen were made in 1997 March and May at the Sutherland site of the South African Astronomical Observatory. The March data were obtained using the 1.0m telescope and the May data using the 0.75m telescope. In both cases the detector was the UCT CCD camera in frame transfer mode (see Stobie et al. 1996). Integration times were 4 and 10 sec for the March data and 20 sec for the May data and the data are all filter-less (ie ‘white-light’). After flat fielding and bias subtraction the images were processed using the DoPHOT package (Mateo & Schechter 1989). Both differential PSF-fit, and aperture, magnitudes were derived (instrumental), corrected for extinction using frame standard stars. On-chip binning (2×2) was used in conditions of poor seeing. The magnitudes are instrumental and we have used the ephemeris of Stobie et al. (1996) to phase the data.

4.1 General light curve features

During our photometric observations in March–May 1997, V895 Cen was observed to increase from an intermediate/low to a high accretion state (Figure 4). This is evident from the increase in the amplitude variation over the orbital cycle and the increased depth of the eclipse. Also, in the observations made in March, there is little evidence of flickering, while flickering becomes quite prominent in cycles 2139 and 2144.

4.2 The eclipse profiles

In Figure 5 we show the light curves centered on the eclipses. The duration, and start and end phase of the eclipse, is constant, taking ~ 26.6 min. This is consistent with the duration of the low/intermediate state data (~ 26.3 min) of Stobie et al (1996). In cycles 1807 and 1812, we observe a rapid eclipse ingress, which takes ~ 40 sec and for the eclipse egress ~ 20 sec. In the succeeding eclipses, the duration of the eclipse ingress becomes progressively longer as a result of the accretion stream brightening, though there is still a rapid decrease in intensity present at the same phase in most cycles.

The resolution of these data is not high enough to resolve the ingress and egress of the accretion region(s) on the white dwarf, which typically take 1–2 sec (cf Perryman et al 2000). We now consider if the duration of the eclipse is consistent with the parameters derived in §3 ($q = 0.5$, $i = 82^\circ$ and $M_1 = 0.9M_\odot$). We assume the Nauenberg (1972) mass-radius relationship for a white dwarf and the secondary is a main sequence star. We determine the size of the eclipsed source by tracing the Roche potential out of the binary system along the line of sight from any point in the vicinity of the white dwarf. We can then measure the eclipse duration for these parameters: they are consistent with the observed eclipse duration. We find no evidence in either these data or in the low state data of Stobie et al (1996) for the presence of an accretion disc. The variable duration of the ingress is due to the gradual eclipse of the accretion stream. As the system becomes brighter, the stream remains visible for a longer duration after the eclipse of the white dwarf.

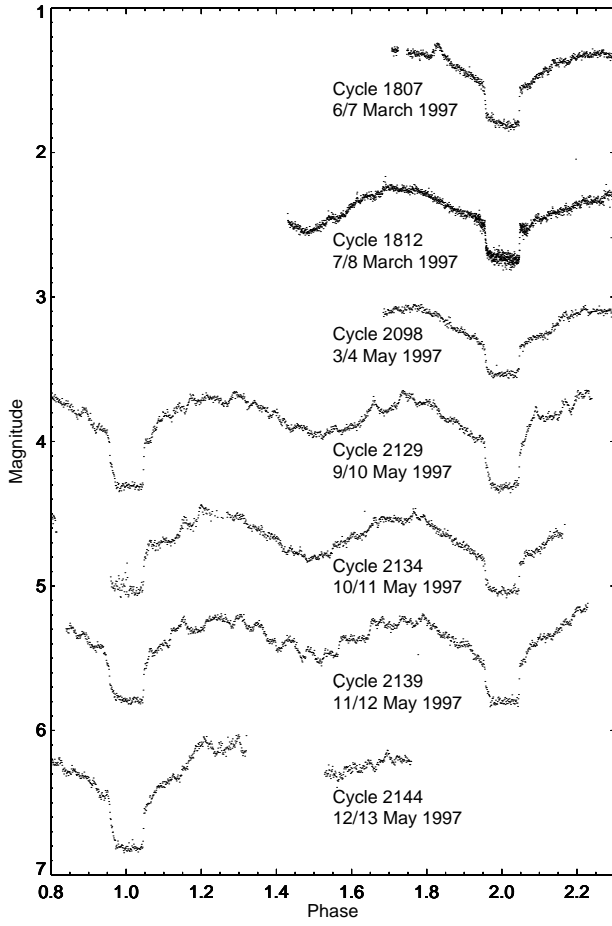


Figure 4. Light curves obtained from the 1997 March 6 to 1997 May 12. The curves have been offset along the y-axis for clarity (since they are instrumental magnitudes the offsets are arbitrary). The cycle number refers to the number of cycles elapsed since the start of the ephemeris of Stobie et al (1996). The integration times for cycle 1807 was 10 sec, 4 sec for cycle 1812 and 20 sec for the May observations.

5 ECLIPSE MAPPING

In the eclipse mapping model of Harrop-Allin et al (1999a, 1999b, 2001) various assumptions have to be made. These include defining the system parameters (such as the masses of the primary and secondary stars), the path of the accretion flow, and whether accretion is occurring onto one or both magnetic poles. The model takes into account the fact that the stream is optically thick using a simple projection factor (the sine of the angle between the line of sight and the tangent to the stream at each point). We assume point-like accretion regions located at the foot-points of the accreting field lines of the white dwarf. In addition the light curves need to be corrected for emission originating from components other than the accretion stream. We address these issues in turn.

5.1 System parameters

The parameters, inclination, i , the coupling radius at which the stream becomes attached to the magnetic field, R_μ , the

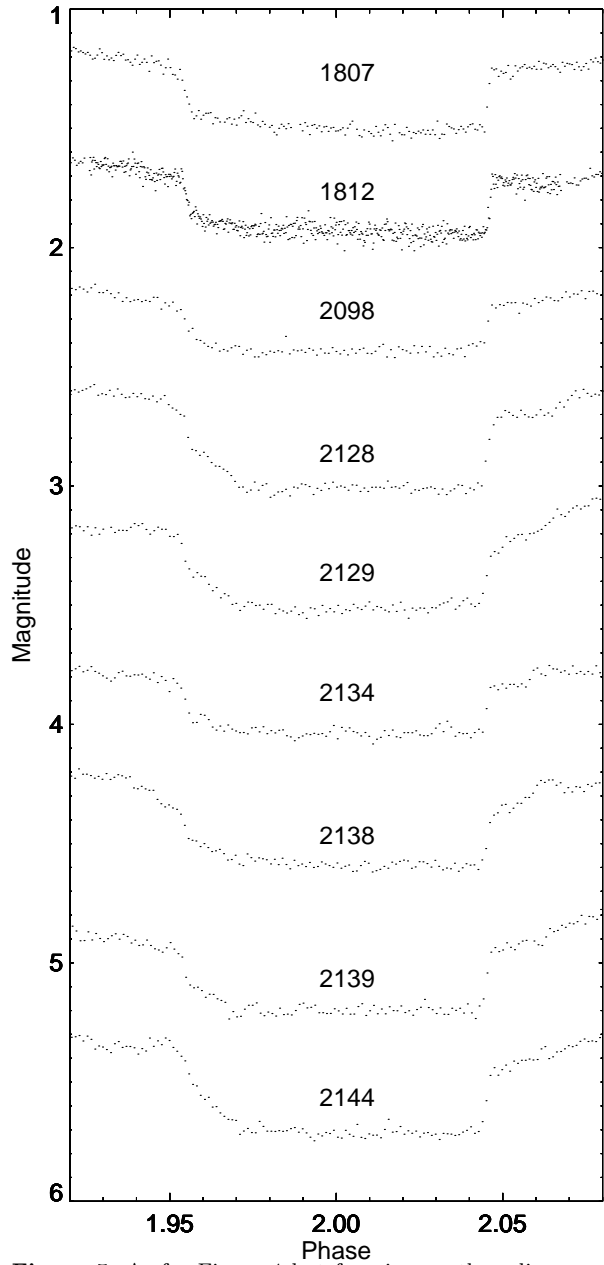


Figure 5. As for Figure 4 but focusing on the eclipse profiles. The integration time for cycle 1807 was 10 sec, cycle 1812 4 sec and 20 sec for the other cycles.

angle between the spin axis and the magnetic axis (the magnetic co-latitude) β and the magnetic longitude ζ of the dipole field line are fitted in the model fit. Since it is an eclipsing system, $i > 72^\circ$ for the above system parameters. From the results in §3 we fix $q=0.51$.

5.2 The smoothing term

Another key parameter used in the fitting process is λ , the Lagrangian multiplier, which determines how smooth the final solution is (Harrop-Allin 1999a). If λ is set too low the model fits noise in the data. If λ is set too high the model smoothes small scale features and the resulting stream images have poor resolution. The appropriate value for our

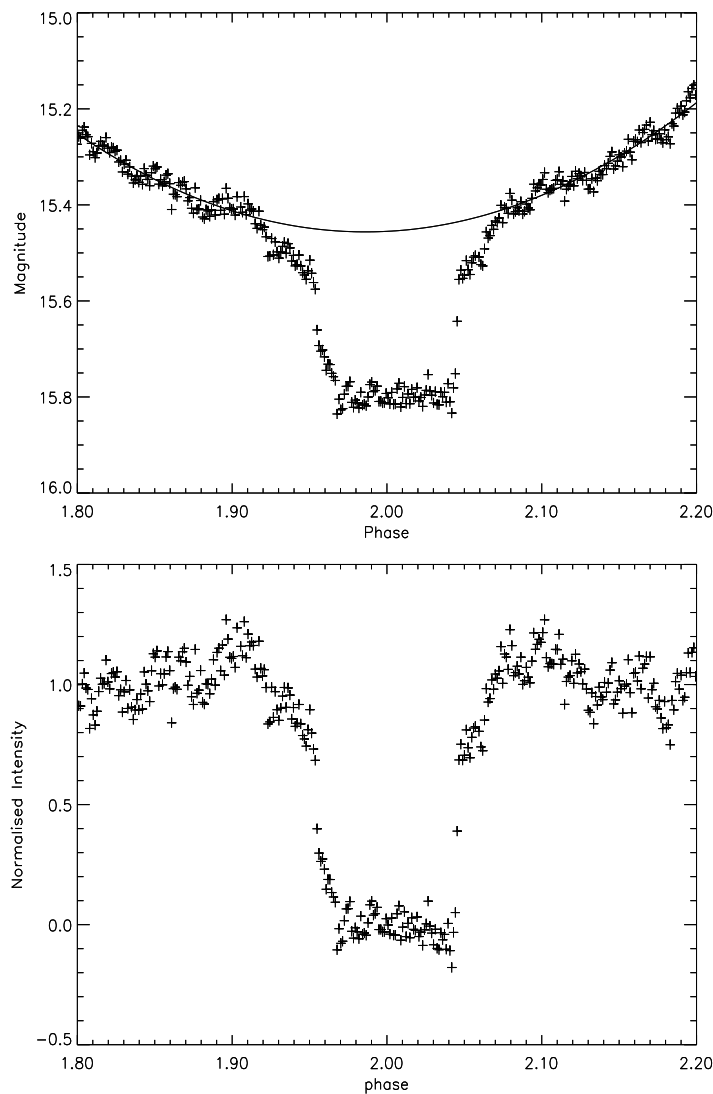


Figure 6. Top panel shows a polynomial fit (degree=2) to the region of the light curve near the eclipse in cycle 2139. The bottom panel shows the normalized eclipse profile.

data with 4 and 10 sec resolution (cycles 1807 & 1812) was found to be $\lambda = 10^5$ and for the data with 20 sec resolution $\lambda = 10^4$. For comparison, Harrop-Allin et al (1999a) found that $\lambda = 10^5$ was appropriate for their test data with 0.7 sec resolution.

5.3 The stream trajectory

One of the assumptions of the model of Harrop-Allin et al (1999a) is the path of the accretion flow: the stream path consists of a ballistic trajectory from the L_1 point to the threading region, after which the stream is forced to follow the magnetic field lines of the white dwarf out of the orbital plane. If the stream deviates significantly from this trajectory, then poor fits to the data are expected.

5.4 Removing non-stream emission

The most important sources of flux in the optical band are the changing viewing angle of the accretion regions on the white dwarf (since cyclotron radiation is strongly beamed), and the accretion stream. The optimum method to subtract the cyclotron component would be to have simultaneous optical polarimetry data since cyclotron emission is polarized. In the absence of such data we have used a very simple approach to subtract the contribution from the accretion region. A polynomial (degree=2) was fitted to the light curves between $\phi \sim 0.8-1.2$ (data from the actual eclipse phases were excluded). The resulting fit was then subtracted from the original data. The normalized eclipse profiles were used as input to the imaging method. The polynomial fit and the results of the orbital trend removal for cycle 2139 are shown in Figure 6. To check if the resulting stream images are sensitive to the way the normalization was made, we also fitted a polynomial to the light curve between other phase intervals (eg $\phi \sim 0.9-1.1$). The resulting stream images were found to be very similar.

Observations of other polars (eg UZ For, Bailey & Cropper 1991) show that the white dwarf photosphere is much fainter in optical light compared with the accretion region. We therefore do not add a separate component to account for the contribution of the white dwarf photosphere to the overall flux.

In our modeling, large errors were assigned to data with phases $\phi < 0.85$ and $\phi > 1.15$ since the accretion stream is fully visible and no useful information can be obtained. This also applies to data occurring at the sharp ingress and egress ($\phi=0.952$ and $\phi=1.046$). This is due to the fact that the model assumes a point source for the emission region rather than a region of any extent.

5.5 One or two pole accretion

It is also necessary to specify whether the stream accretes onto one or both foot points of the magnetic dipole field line. Harrop-Allin et al. (1999a) found that if a one-pole model is applied to a two pole geometry the resulting fit will be very poor. Applying a two-pole model to a one-pole geometry gave fits with high χ^2/N but produced stream images with brightness concentrated on the upper stream. Given data of sufficient quality, it is therefore possible to determine whether to use a one-pole geometry or a two-pole geometry simply on the basis of the model fits alone. We performed model fits using both one pole and two pole geometry. In the one pole geometry poor fits were obtained, $\chi^2/N \sim 10-20$. In contrast, a two pole geometry gave good fits, with $\chi^2/N \sim 1$. A two-pole geometry was therefore applied.

6 ECLIPSE MAPPING RESULTS

The goodness of the model fit to the data is more strongly dependent on some parameters than others. The duration of the eclipse is controlled mainly by q and i . For various combinations of (q, i) , equally good fits were obtained. We found that $q=0.51$ and $i = 82^\circ$ (cf §3) gave good fits to data from all the cycles: we therefore fixed these parameters at

Cycle	β	ζ	R_μ	χ^2/N
1807	11.5	85	0.24a (42 R_{wd})	0.42
1812	11.5	85	0.23a (40 R_{wd})	0.90
2098	11.5	85	0.23a (40 R_{wd})	0.71
2128	10.5	85	0.27a (47 R_{wd})	0.39
2129	10.0	85	0.27a (47 R_{wd})	0.69
2134	11.5	85	0.25a (43 R_{wd})	0.67
2138	12.0	85	0.27a (47 R_{wd})	0.24
2139	12.0	85	0.26a (45 R_{wd})	1.50
2144	10.0	85	0.27a (47 R_{wd})	0.27

Table 1. The results of our model fits to the data. We show the best fits to the latitude of the magnetic axis β , the magnetic longitude, ζ , and the radius from the white dwarf that the stream gets controlled by the magnetic field, R_μ . We also show the goodness of fit. In the above results we have used $q = 0.51$, $i = 82^\circ$.

these values. For these parameters, the angle of the magnetic axis, β , was found to be $\beta = 11^\circ \pm 1^\circ$. The magneto-spheric radius, R_μ , was primarily determined by the phase at which the stream was fully eclipsed. This uncertainty in this parameter was estimated to be $\pm 0.05a$. The uncertainty in β and R_μ is based on the range of values for which χ^2 remains unchanged. We caution that similar χ^2/N values could be obtained for a larger range of values of β and R_μ for a different combination of input parameters.

Changing the magnetic longitude, ζ , by $\pm 10^\circ$ had no significant change on the phase at which the model reached totality. A constant value of $\zeta = 85^\circ$ has been used for imaging all cycles. We show the best fit results of our modeling in table 1: good fits were obtained to the data from all the cycles except cycle 2139 where $\chi^2_\nu = 1.50$.

We obtained corresponding images of the accretion stream for all our model fits. As these stream images are similar for certain cycles we only show three of them (along with their model eclipse profiles) in Figure 7. In selecting the images to present, we considered which of the cycles had the best quality data and sampled various intensity states. For instance in cycle 1812, the system was in an intermediate/low accretion state and also had data with the highest time resolution (4 sec) of any of our data. We also show cycle 2144 since V895 Cen was in its highest accretion state that we observed photometrically. Intermediate in epoch and accretion state are cycles 2128, 2129, 2138 and 2139: since cycle 2138 gave the best fit (table 1), we also show the stream map for this cycle.

In cycles 1807, 1812 and 2098, V895 Cen was in an intermediate/low accretion state. Our results show that the accretion stream brightens rapidly nearer to the white dwarf. (Since our photometry was differential rather than absolute, our maps do not allow us to compare the brightness of the stream from cycle to cycle). There is no appreciable enhancement in emission either at R_μ or in the ballistic stream component. As V895 Cen enters a higher accretion state, the stream brightens along the full extent of the magnetically controlled stream in both the upper and lower field lines. In our last cycle (2144) the system is in the highest accretion state - as inferred from the largest eclipse depth and peak to peak variation. In this cycle, our model suggests that emission is now concentrated along the field lines originating from the upper pole.

7 DISCUSSION

7.1 The eclipsed source

Stobie et al (1996) suggested that the eclipsed component was not the white dwarf. This was based on the fact that the eclipse occurred before the secondary minimum in the light curve. Assuming the secondary minimum was the true marker of inferior conjunction, and taking the timings of the eclipse ingress and egress relative to this, they concluded that the eclipsed source was ~ 30 white dwarf radii from the white dwarf. We have found that the phasing of the eclipse ingress and egress occurs at exactly the same orbital phase in both low, intermediate and high state data (cf Figure 5). If the eclipsed source was the stream as suggested by Stobie et al (1996) we would not expect to observe the stability in the eclipse features as we do.

We now address the fact that the eclipse appears off-set from the secondary minimum in the low state light curves of Stobie et al (1996). Many polars show evidence for heating of the trailing face of the secondary by the accretion region on the white dwarf. It is expected that even if the irradiation is sharply reduced or switched off, the trailing face of the secondary will remain heated for some duration. Szkody et al (1999) estimate that in the case of the polar AR UMa it takes around 5 months for the secondary to cool down to the temperature of the unheated part of the star. Indeed, from our Doppler tomography results (§3) we find that the secondary in V895 Cen is still heated when we observed it in a low accretion state. This has the effect of increasing the optical flux between $\phi=0.5-0.9$ compared to a secondary star with no irradiation. We suggest that the apparent offset between the eclipse and the secondary minimum is due to asymmetric irradiation of the secondary star.

7.2 The indirect stream mapping results

Our results show that in the intermediate/low accretion state the stream brightens rapidly as it nears the white dwarf. In our brightest state data, we find that stream emission is concentrated mainly along the field lines leading to the upper pole. At face value this suggests that as the system reaches a high enough mass transfer rate, the accretion mode goes from a two-pole to a one-pole model. It is not clear why this would be the case, but it suggests that with an increase in the mass transfer rate, the upper pole is now the more favorable pole to accrete.

In all our model fits, there is no evidence for a brightening of the accretion stream at the magneto-spheric interaction region. These results are similar to that of the low accretion state data of HU Aqr (Harrop-Allin et al. 2001). However, there was some indication that the stream brightened at the interaction region in the U and B bands. Using emission line data of HU Aqr in a high accretion state and a different technique to that used here, Vrielmann & Schwöpe (2001) derived stream brightness maps and found a brightening of the stream in the magneto-spheric interaction region of HU Aqr. It is possible that the accretion state (and hence amount of irradiation) plays an important role in determining whether the stream is found to brighten at the interaction region.

It is interesting to compare the coupling radius that we

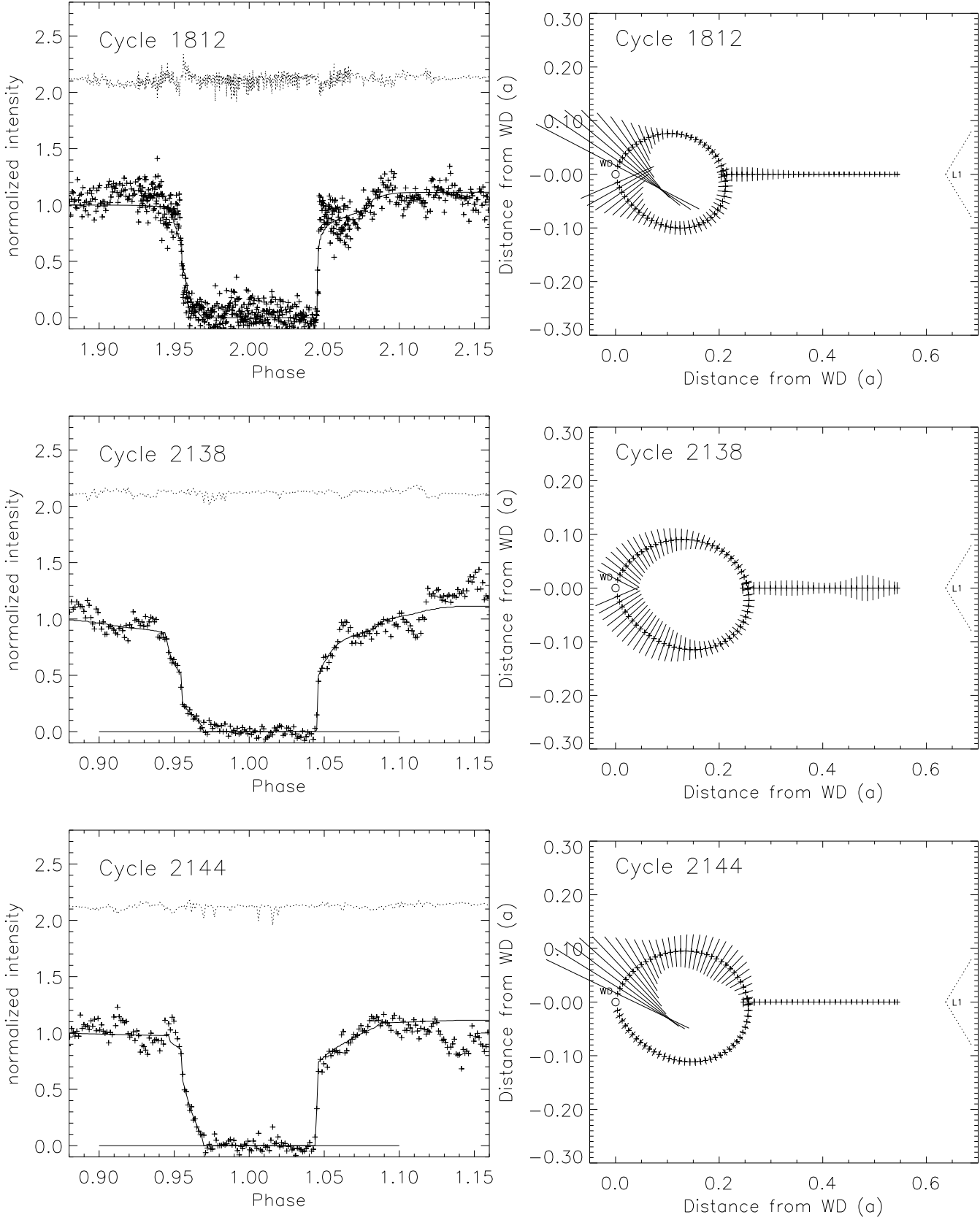


Figure 7. Model eclipse profiles and the corresponding accretion stream images for three orbital cycles. The stream images are shown projected onto a plane passing through the center of both stars and perpendicular to the orbital plane. The brightness of each emission point is shown as a line perpendicular to the stream and passing through the point; the brightness of the point is represented by the length of the line. The white dwarf is shown to scale as a circle (labeled 'WD'), and the secondary is shown (not to scale) to mark the position of the L1 point (labeled 'L1').

derive from our model fits with that of HU Aqr (Harrop-Allin 1999b, 2000). They find that in a high accretion state, $R_\mu \sim 0.18a$. We find a mean value of $R_\mu \sim 0.25$ from our fits. HU Aqr has a magnetic field strength of 36 MG (Schwope, Thomas & Beuermann 1993). Since we expect the accretion flow to interact with the magnetic field when the magnetic pressure equals the ram pressure of the flow, we predict that the magnetic field strength of V895 Cen is significantly larger than that of HU Aqr, other things (such as \dot{M}) being equal.

8 SUMMARY

We find from our photometric data that the eclipsed component is consistent with the accretion regions on the white dwarf. Our indirect imaging results suggest that the stream brightens close to the magnetic poles in the low/intermediate accretion state. In the highest accretion state we observe, emission is extended along the field lines leading to the upper magnetic pole.

9 ACKNOWLEDGMENTS

We would like to thank Kate Harrop-Allin and Henk Spruit for the use of their software and the Australian National University for the generous allocation of observing time.

REFERENCES

Bailey, J., Cropper, M., 1991, MNRAS, 253, 27
 Baraffe, I., Kolb, U., 2000, MNRAS, 318, 354
 Craig N., Howell S.B., Sirk M.M., Malina R.F., 1996, ApJ, 457, 191
 Hakala P.J., 1995, A&A, 296, 164
 Harrop-Allin M. K., Hakala P.J., Cropper M., 1999a, MNRAS, 302, 362 (Paper I)
 Harrop-Allin M. K., Hakala P.J., Cropper M., Hellier C., Ramsseyer T., 1999b, MNRAS, 308, 807 (Paper II)
 Harrop-Allin M. K., Potter, S. B., Cropper M., accepted, MNRAS (Paper III)
 Howell, S. B., Craig, N., Roberts, B., McGee, P., Sirk M., 1997, AJ, 113, 2231
 Lubow S. H., Shu F. H., 1975, ApJ, 198, 383
 Mateo M., Schechter P.L., 1989, In Proc 1st. ESO/ST-ECF Data Analysis Workshop, Editors: P.J. Grosbol, F. Murtagh, R.H. Warmels, ESO, Garching, Germany
 Mukai K., 1988, MNRAS, 232, 135
 Perryman, M. A. C., Cropper, M., Ramsay, G., Favata, F., Peacock, A., Rando, N., Reynolds, A., accepted, MNRAS
 Schwope A.D., Thomas, H. C., Beuermann, K., 1993, A&A, 271, L25
 Schwope A.D., Mantel, K.-H., Horne, K., 1997, A&A, 319, 894
 Spruit, H. C., 1998, astro-ph/9806141
 Stobie R.S., Okeke P.P., Buckley D.A.H., O'Donoghue D., 1996, MNRAS, 283, L127
 Szkody, P., Vennes, S., Schmidt, G. D., Wagner, M., Fried, R., Shafter, A. W., Fierce, E., 1999, ApJ, 520, 841
 Vrielmann, S., Schwope, A. D., 2001, 322, 269
 Warner B., 1995, Cataclysmic variable stars, Cambridge Univ. Press, Cambridge
 Wu, K., 2000, Space Sci Rev, 93, 611